BBA - Molecular Basis of Disease 1864 (2018) 1653–1662

Contents lists available at ScienceDirect

BBA - Molecular Basis of Disease

journal homepage: www.elsevier.com/locate/bbadis

# Herpud1 impacts insulin-dependent glucose uptake in skeletal muscle cells by controlling the $Ca^{2+}$-calcineurin-Akt axis

Mario Navarro-Marquez[a], Natalia Torrealba[a], Rodrigo Troncoso[a,b], Cesar Vásquez-Trincado[a], Marcelo Rodriguez[a], Pablo E. Morales[a], Elisa Villalobos[a,e], Yuka Eura[c], Lorena Garcia[a], Mario Chiong[a], Amira Klip[d], Enrique Jaimovich[a], Koichi Kokame[c], Sergio Lavandero[a,e,*]

[a] Advanced Center for Chronic Diseases (ACCDIS) & Center for Exercise, Metabolism & Cancer (CEMC), Faculty of Chemical & Pharmaceutical Sciences & Faculty of Medicine, University of Chile, Santiago, Chile
[b] Institute for Nutrition & Food Technology (INTA), University of Chile, Santiago, Chile
[c] Department of Molecular Pathogenesis, National Cerebral and Cardiovascular Center, Suita, Osaka, Japan
[d] Cell Biology Programme, The Hospital for Sick Children & Department of Physiology, University of Toronto, Toronto, Canada
[e] Department of Internal Medicine (Cardiology Division), University of Texas Southwestern Medical Center, Dallas, TX, USA

ARTICLE INFO

*Keywords:*
Herpud1
Insulin
Akt
Calcium
Calcineurin
Skeletal muscle

ABSTRACT

Skeletal muscle plays a central role in insulin-controlled glucose homeostasis. The molecular mechanisms related to insulin resistance in this tissue are incompletely understood. Herpud1 is an endoplasmic reticulum membrane protein that maintains intracellular $Ca^{2+}$ homeostasis under stress conditions. It has recently been reported that *Herpud1*-knockout mice display intolerance to a glucose load without showing altered insulin secretion. The functions of Herpud1 in skeletal muscle also remain unknown. Based on these findings, we propose that Herpud1 is necessary for insulin-dependent glucose disposal in skeletal muscle. Here we show that Herpud1 silencing decreased insulin-dependent glucose uptake, GLUT4 translocation to the plasma membrane, and Akt $Ser^{473}$ phosphorylation in cultured L6 myotubes. A decrease in insulin-induced Akt $Ser^{473}$ phosphorylation was observed in *soleus* but not in *extensor digitorum longus* muscle samples from *Herpud1*-knockout mice. Herpud1 knockdown increased the $IP_3R$-dependent cytosolic $Ca^{2+}$ response and the activity of $Ca^{2+}$-dependent serine/threonine phosphatase calcineurin in L6 cells. Calcineurin decreased insulin-dependent Akt phosphorylation and glucose uptake. Moreover, calcineurin inhibition restored the insulin response in Herpud1-depleted L6 cells. Based on these findings, we conclude that Herpud1 is necessary for adequate insulin-induced glucose uptake due to its role in $Ca^{2+}$/calcineurin regulation in L6 myotubes.

## 1. Introduction

Skeletal muscle insulin resistance is an early finding in the progression to type 2 diabetes mellitus [1]. The molecular mechanisms underlying the altered insulin response remain unclear. The homocysteine-inducible endoplasmic reticulum (ER) protein with ubiquitin-like domain 1 (Herpud1), an ER membrane protein, is ubiquitously expressed and highly inducible under stress conditions [2,3]. Eura et al. reported that *Herpud1*-knockout (KO) mice show poor glucose tolerance but normal levels of insulin secretion [4]. Given that skeletal muscle is largely responsible for glucose uptake under postprandial conditions [5], Herpud1 may regulate insulin-dependent glucose uptake in this tissue. Prior studies have shown that Herpud1 protects against cell death through stabilization of inositol 1,4,5-trisphosphate receptor (IP3R)-dependent $Ca^{2+}$ signaling under stress conditions [6–8]. We have also previously demonstrated the importance of the $IP_3R$-induced $Ca^{2+}$ response for adequate insulin-induced glucose uptake [9–12]. Therefore, we hypothesize that Herpud1 knockdown disrupts $Ca^{2+}$ homeostasis and alters intracellular signaling pathways regulated by $Ca^{2+}$.

Calcineurin is a $Ca^{2+}$-dependent serine/threonine phosphatase [13]. Ni et al. have previously shown that calcineurin decreases insulin-

*Abbreviations:* AdLacZ, adenovirus encoding β-galactosidase; CAIN, calcineurin inhibitor; CA-CN, constitutively-active calcineurin; CsA, cyclosporine A; [$^3$H]-2DG, [$^3$H]2-deoxyglucose; ER, endoplasmic reticulum; KO, knockout; Herpud1, homocysteine-inducible endoplasmic reticulum protein with ubiquitin-like domain 1; IR, insulin receptor; $IP_3R$, 1,4,5-trisphosphate receptor; OPD, *o*-phenylenediamine; PI, propidium iodide; siRNA, small interfering RNA

* Corresponding author at: Advanced Center for Chronic Diseases (ACCDIS) & Center for Exercise, Metabolism & Cancer (CEMC), Faculty of Chemical & Pharmaceutical Sciences & Faculty of Medicine, University of Chile, Santiago, Chile.
*E-mail address:* slavander@uchile.cl (S. Lavandero).

https://doi.org/10.1016/j.bbadis.2018.02.018
Received 13 October 2017; Received in revised form 17 February 2018; Accepted 20 February 2018
Available online 24 February 2018
0925-4439/ 

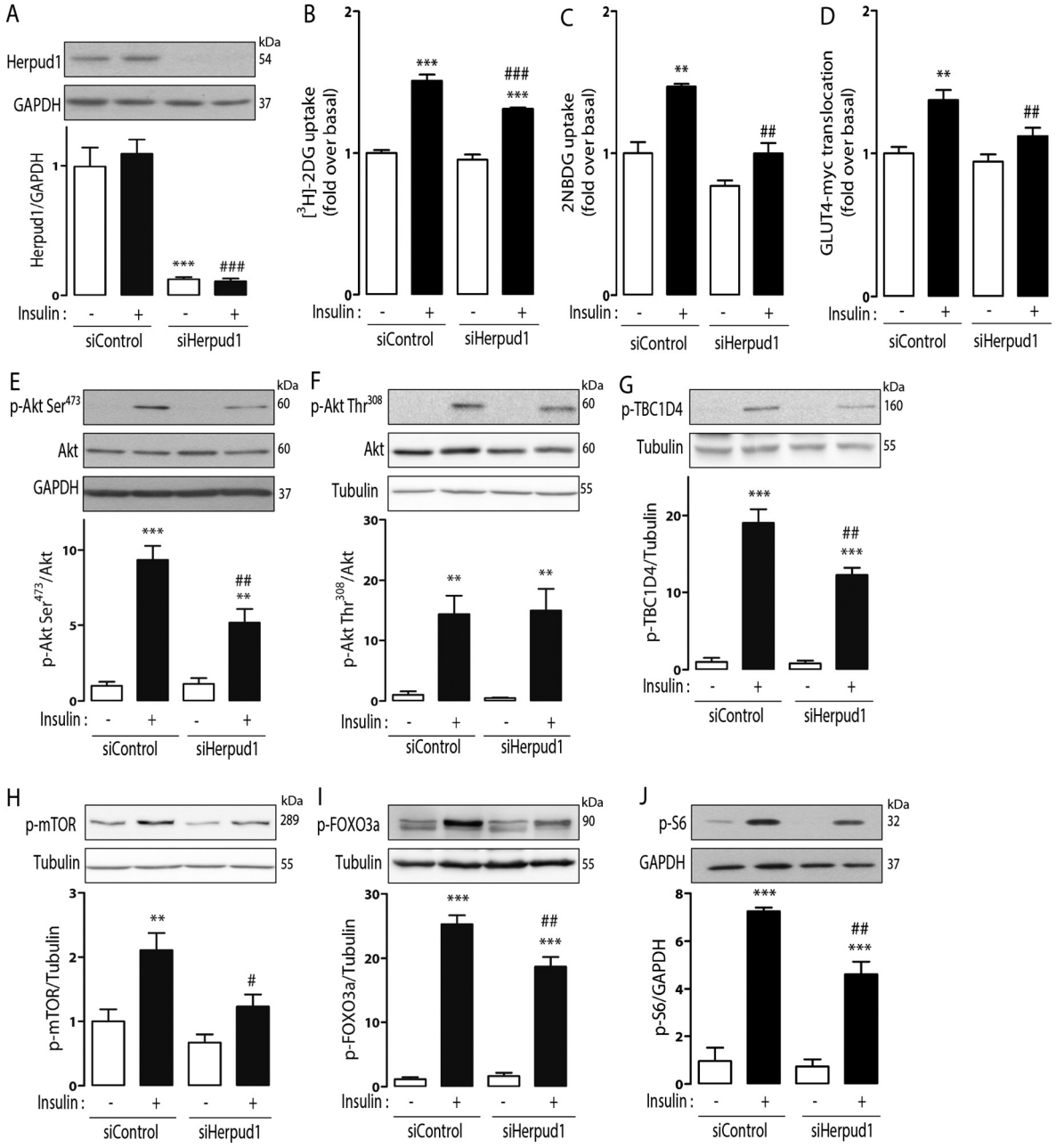


**Fig. 1.** Herpud1 regulates insulin-induced glucose uptake in skeletal muscle cells. (A) Top panel: representative Western blot of Herpud1 protein levels in siControl and siHerpud1 L6 myotubes. Bottom panel: densitometric quantification (mean ± SEM; $n = 3$). (B) Effect of Herpud1 knockdown on [$^3$H]-2DG uptake (mean ± SEM; $n = 3$). (C) Effect of Herpud1 knockdown on 2-NBDG uptake in siControl and siHerpud1 cells (mean ± SEM; $n = 3$). (D) OPD assay showing the effect of Herpud1 knockdown on GLUT4 plasma membrane translocation (mean ± SEM; $n = 4$). (E–J) Top panels: representative Western blots showing the effects of Herpud1 silencing on basal and insulin-induced (E) Akt Ser$^{473}$ phosphorylation (mean ± SEM; $n = 4$), (F) Akt Thr$^{308}$ phosphorylation (mean ± SEM; $n = 5$), (G) TBC1D4 Thr$^{642}$ phosphorylation (mean ± SEM; $n = 4$), (H) mTOR Ser$^{2448}$ phosphorylation (mean ± SEM; $n = 5$), (I) FOXO3a Thr$^{32}$ phosphorylation (mean ± SEM; $n = 6$) and S6 Ser$^{235/236}$ phosphorylation (mean ± SEM; $n = 3$). Bottom panels: densitometric analysis. $^{**}p < 0.01$, $^{***}p < 0.001$ versus basal condition; $^{\#}p < 0.05$, $^{\#\#}p < 0.01$, $^{\#\#\#}p < 0.001$ between insulin-stimulated conditions. One-way ANOVA followed by Tukey's *post hoc* test.

induced Akt phosphorylation in cultured cardiomyocytes [14]. This phosphatase is important in skeletal muscle hypertrophy, but its role in insulin signaling in this tissue remains unknown [15,16]. Given the above findings, we propose that Herpud1 controls insulin-dependent glucose uptake through the regulation of $Ca^{2+}$-dependent serine-threonine phosphatase calcineurin. Our results show that Herpud1 silencing decreases insulin-triggered glucose uptake, GLUT4 translocation to the plasma membrane, and Akt Ser$^{473}$ phosphorylation in L6 myotubes. This finding is consistent with an amplified $IP_3R$-dependent cytosolic $Ca^{2+}$ response and increased calcineurin activity. We also observed that calcineurin regulates insulin response in L6 myotubes and that Akt Ser$^{473}$ phosphorylation after insulin stimulation was depressed in soleus but not in extensor digitorum longus (EDL) muscle from *Herpud1*-KO mice. Finally, calcineurin inhibition restores insulin-induced glucose uptake in Herpud1-depleted L6 myotubes.

## 2. Material and methods

### 2.1. Reagents

Insulin (I0516), histamine (H7250), cyclosporine A (30024), fetal bovine serum (F2442), *o*-phenylenediamine (P5412), phosphatase inhibitors (P2726), protease inhibitors (11836170001), scramble (SIC001) and Herpud1 (SASI_Hs01_00185592) small interfering RNA

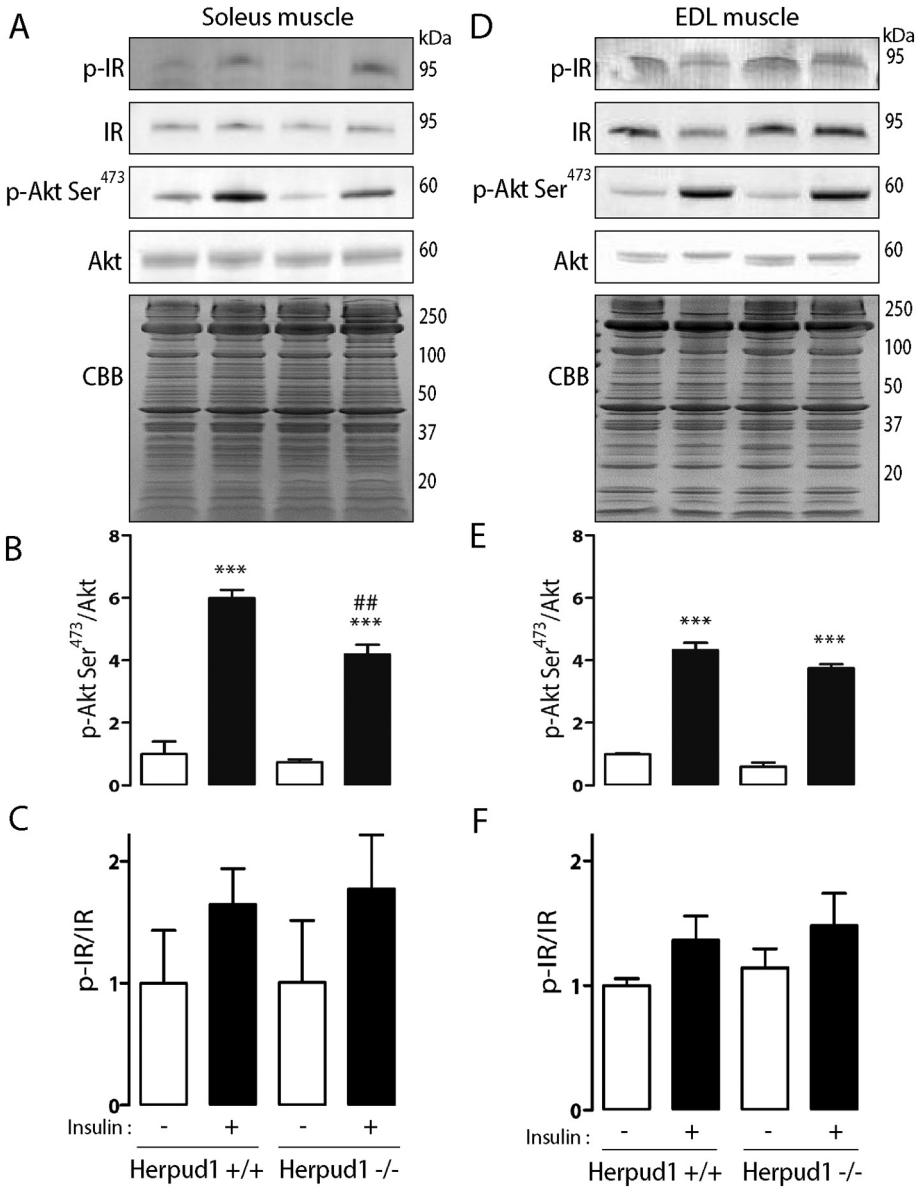


**Fig. 2.** Altered insulin response in skeletal muscle of *Herpud1*$^{-/-}$ mice. *Herpud1*$^{+/+}$ and *Herpud1*$^{-/-}$ mice were fasted for 12 h and then stimulated with insulin 1 U/kg for 7.5 min. EDL and soleus muscles were isolated and frozen at −80 °C. (A) Representative Western blot of soleus muscle in control and *Herpud1*-KO mice. (B) Quantification of Akt Ser$^{473}$ phosphorylation (mean ± SEM; $n = 3$). (C) Quantification of IR Tyr$^{1361}$ phosphorylation (mean ± SEM; $n = 3$). (D) Representative Western blot of EDL muscle in control and *Herpud1*-KO mice. (E) Densitometric analyses of Akt Ser$^{473}$ phosphorylation (mean ± SEM; $n = 3$). (F) Quantification of IR Tyr$^{1361}$ phosphorylation (mean ± SEM; $n = 3$). CBB: Coomassie brilliant blue. $^{***}p < 0.001$ between basal conditions; $^{\#\#}p < 0.01$ between insulin-stimulated conditions. One-way ANOVA followed by Tukey's *post hoc* analysis.

(siRNA), and RCAN1 (SAB2101967) and c-Myc (3956; 1:500 dilution) antibodies were obtained from Sigma-Aldrich. Opti-MEM (31985070), alpha-MEM (11900024), oligofectamine (12252-011), lipofectamine 2000 (11668019), 2-NBDG (N13195), fura-2 AM (F1201), fluo-4 AM (F14201), rhod-FF AM (R23983), BCA Protein Quantification Kit (23225), and $IP_3R2$ (PA1-904) antibodies were from Thermo-Fisher Scientific. Primary antibodies *p*-Akt Ser$^{473}$ (sc-4060; 1:2000 dilution), *p*-Akt Thr$^{308}$ (sc-9275; 1:1000 dilution), Akt (sc-2966; 1:1000 dilution), *p*-IR Y$^{1361}$ (sc-3023; 1:1000 dilution), IR (sc-3020; 1:1000 dilution), *p*-TBC1D4 (#4288; 1:1000 dilution), *p*-mTOR (#2971; 1:1000 dilution) and *p*-FOXO (#9464; 1:1000 dilution) and *p*-S6 Ser$^{235/236}$ (sc-4858; 1:2000 dilution) were from Cell Signaling Technology. Herpud1 (BML-PW9705; 1:50,000 dilution) antibody was from Enzo Life Sciences. Primary antibodies for pan-$IP_3R$ (Ab111087; 1:1000 dilution) were from Abcam. The EZ-ECL enhanced chemiluminescence detection kit for HRP (20-500-1000), trypsin EDTA 10× (03-051-5B) and penicillin-streptomycin-amphotericin B solution (03-033-1B) were from Biological Industries. 2-Deoxy-D-glucose (25972), HRP-conjugated goat anti-mouse secondary antibodies (12-349; 1:5000 dilution), and goat anti-rabbit (AP307P; 1:5000 dilution) were from Calbiochem. $IP_3R1$ (AB5882) antibody was from Merck Millipore. $IP_3R3$ (610313) antibody was from BD Bioscience.

### 2.2. Herpud1-KO mice

*Herpud1*$^{-/-}$ KO (10–12 week old) male mice were developed by Dr. Koichi Kokame (National Cerebral and Cardiovascular Center, Osaka) as previously described [4]. All animals were handled in accordance with the eighth edition of the National Institutes of Health Guide for the Care and Use of Laboratory Animals. All experimental protocols were approved by the Bioethics Committee, Faculty of Chemical and Pharmaceutical Sciences, University of Chile (#BE2014-01).

### 2.3. Insulin stimulation in vivo

Adult *Herpud1*$^{-/-}$ and control mice were fasted for 12 h and then given an intraperitoneal injection of insulin (1 U/kg) diluted in saline, as previously described [17,18]. After 7.5 min, the mice were sacrificed and the *soleus* and *extensor digitorum longus* (EDL) muscles isolated, frozen in liquid nitrogen, and stored at −80 °C until analysis.

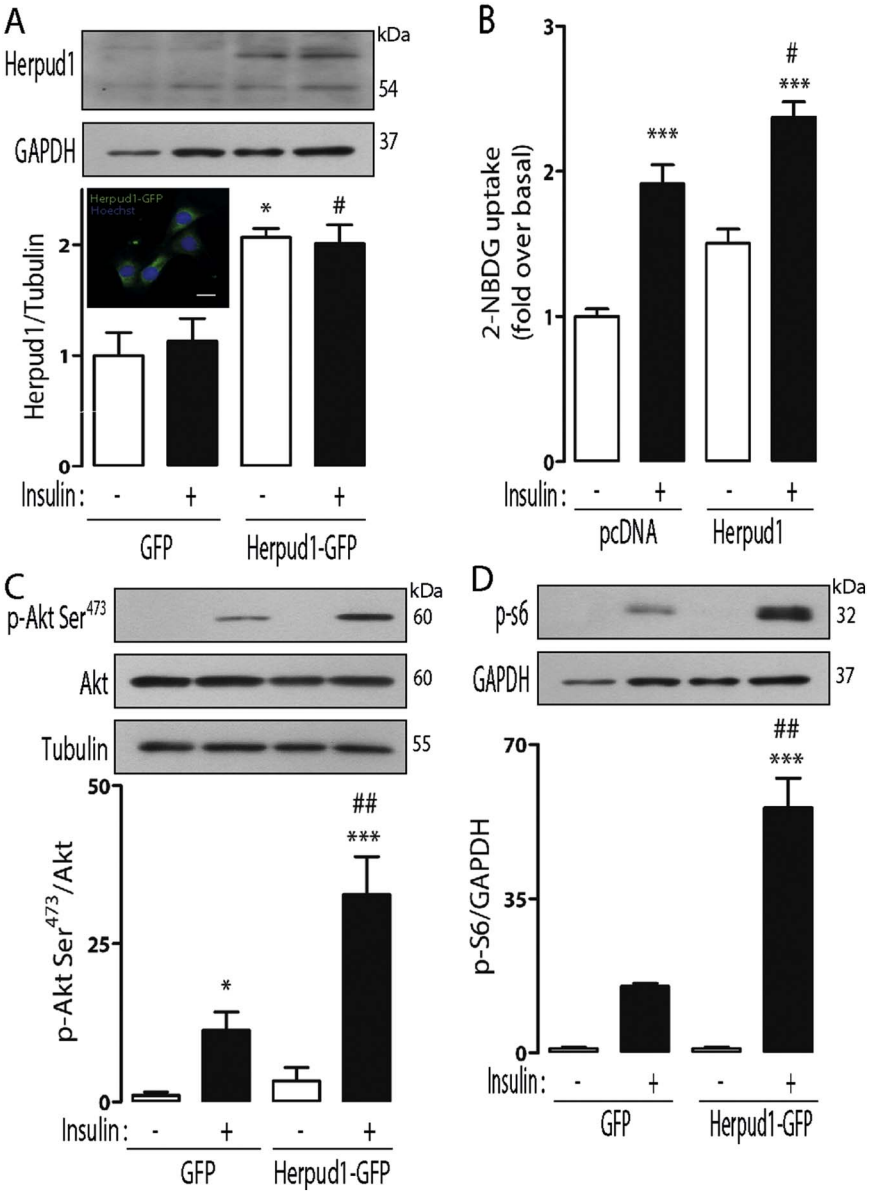


**Fig. 3.** Effect of Herpud1 overexpression in insulin-dependent glucose uptake in L6 myotubes. (A) Top panel: representative Western blot of Herpud1 levels in GFP- and Herpud1-GFP-transfected L6 myotubes. Bottom panel: Densitometric analysis of immunoblots (mean ± SEM; $n = 3$). Insert: Representative immunofluorescence showing expression of Herpud1-GFP in L6 myoblasts (scale bar: 10 μm) (B) 2-NBDG uptake in control (pcDNA) or Herpud1-overexpressed (Herpud1) cells (mean ± SEM; $n = 3$). (C) Top panel: representative Western blot of Akt $Ser^{473}$ phosphorylation in GFP and Herpud1-GFP transfected cells. Bottom panel: densitometric quantification (mean ± SEM; $n = 3$). (D) Top panel: S6 $Ser^{235/236}$ phosphorylation levels in GFP- and Herpud1-GFP-transfected L6 myotubes; representative image. Bottom panel: densitometric analysis (mean ± SEM; $n = 3$). $^{*}p < 0.05$, $^{***}p < 0.001$ between basal conditions; $^{\#}p < 0.05$, $^{\#\#}p < 0.01$, between insulin-stimulated conditions. One-way ANOVA followed by Tukey's *post hoc* test.

### 2.4. Cell culture

Wild-type L6 skeletal muscle cells and L6 muscle cells stably expressing GLUT4 with a Myc epitope in the first extracellular loop (L6-GLUT4myc) [19] were cultured in alpha-MEM supplemented with 10% (v/v) fetal bovine serum (FBS) and 1% (v/v) penicillin-streptomycin-amphotericin B solution in a humidified atmosphere with 5% $CO_2$ at 37 °C. For differentiation, cells were incubated in alpha-MEM supplemented with 2% (v/v) FBS for 5–7 days.

### 2.5. Small interfering RNA (siRNA) silencing

L6 cells were transfected with 100 nM control-scrambled siRNA or *Herpud1* siRNA using oligofectamine transfection reactive according to manufacturer instructions. Experiments were carried out 48 h after transfection. The extent of knockdown was assessed by immunoblotting.

### 2.6. Adenovirus transduction

Myotubes were transduced with calcineurin inhibitor (CAIN) and constitutively-active calcineurin (CA-CN) adenoviral vectors, at a multiplicity of infection (MOI) of 1000, 48 h before experiments. Adenovirus encoding β-galactosidase (AdLacZ) was used as a control.

### 2.7. Plasmid transfection

L6 myotubes were transfected with 1 μg of GFP, *Herpud1*-GFP, pcDNA3.1, or *Herpud1* (mouse) plasmids using 5 μL/mL of lipofectamine 2000. Myotubes were incubated for 6 h with the transfection mixture in Opti-MEM and then for 48 h in alpha-MEM 2% FBS prior to experiments.

### 2.8. [$^3$H]-2Deoxyglucose ([$^3$H]-2DG) uptake

Glucose uptake was measured using 10 μM [$^3$H]2-deoxyglucose ([$^3$H]-2DG) solution for 10 min at 37 °C, as previously reported [20]. Myotubes were serum starved for 3 h and stimulated with insulin (100 nM) for 20 min at 37 °C. Radioactivity was determined by liquid scintillation counting.

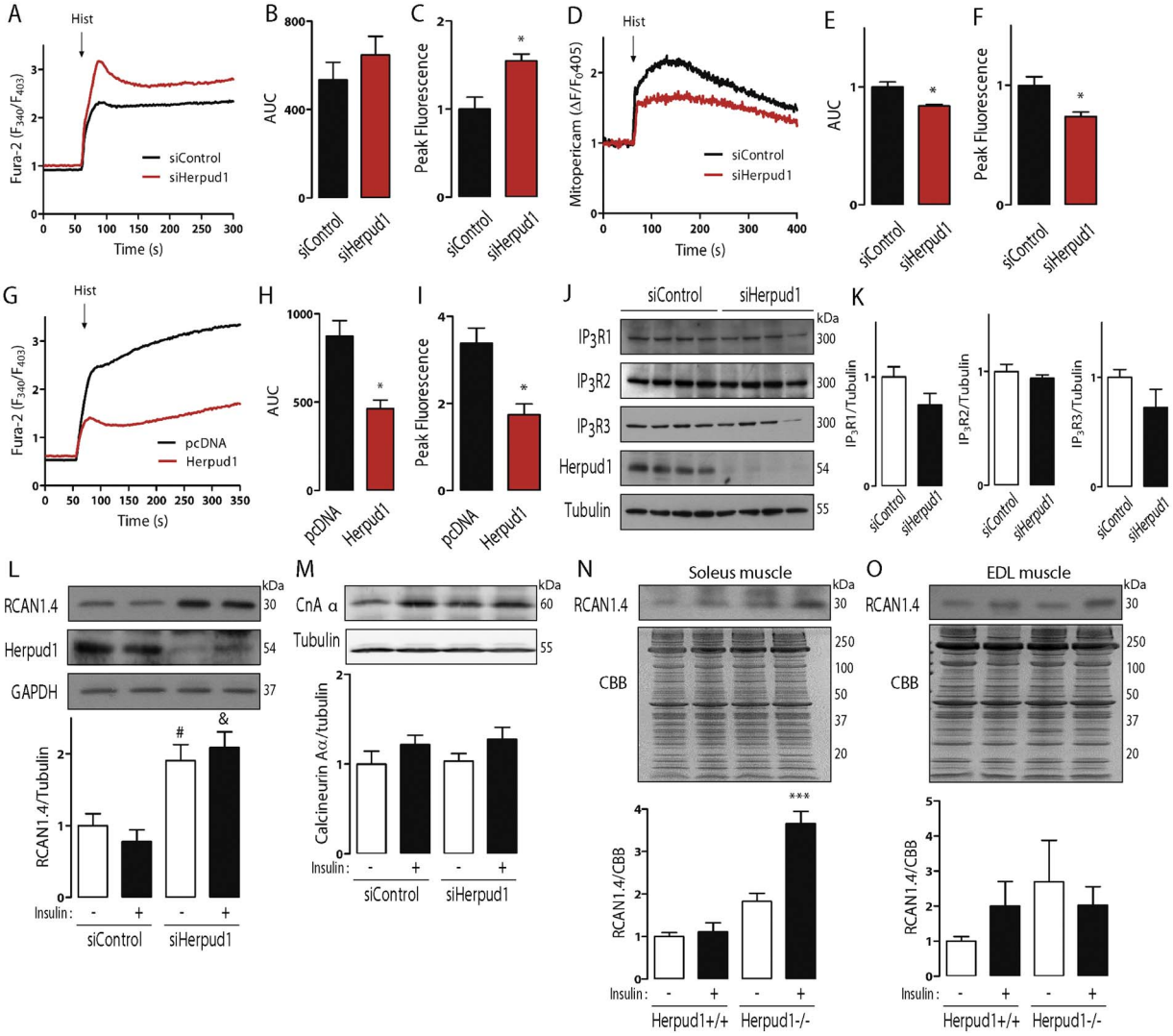


**Fig. 4.** Herpud1 regulates $Ca^{2+}$ homeostasis and calcineurin activity in L6 myotubes. Cytosolic and mitochondrial $Ca^{2+}$ levels were evaluated in siControl and siHerpud1 L6 myotubes. After 60 s of basal measurement, cells were stimulated with histamine (100 μM). (A) Cytosolic $Ca^{2+}$ kinetic using fura-2-AM as a $Ca^{2+}$ indicator (mean; $n = 3$). (B) Area under the curve (AUC) after histamine stimulation (mean ± SEM; $n = 3$). (C) Quantification of peak fluorescence (mean ± SEM; $n = 3$). (D) Kinetics of mitochondrial calcium levels in siControl and siHerpud1 L6 myotubes transfected with genetically-encoded $Ca^{2+}$ indicator mito-pericam (mean; $n = 3$). (E) AUC for the histamine-induced $Ca^{2+}$ response (mean ± SEM; $n = 3$). (F) Histamine-induced peak fluorescence (mean ± SEM; $n = 3$). $^{*}p < 0.05$ between conditions after *t*-test. (G) Kinetics of cytosolic $Ca^{2+}$ response in control (pcDNA) and Herpud1 overexpressed conditions (Herpud1), using fura-2-AM as a $Ca^{2+}$ indicator (mean; $n = 3$). (H) AUC and (I) peak response of kinetics showed in (G). $^{*}p < 0.05$ between conditions after *t*-test. (J) Western blot showing the effect of Herpud1 knockdown on $IP_3R$ isoform 1, 2, and 3 protein levels. (K) Densitometric analysis of immunoblots (mean ± SEM; $n = 4$). (L) Top panel: Effect of Herpud1 silencing on RCAN1.4 expression (representative image). Bottom panel: Densitometric analysis of RCAN1.4 protein levels. $^{\#}p < 0.05$ between basal conditions. $^{\&}p < 0.05$ between insulin-stimulated conditions after one-way ANOVA followed by Tukey's *post hoc* test. (M) Protein levels of calcineurin Aα (CnAα; mean ± SEM; $n = 7$). (N–O) Protein levels of RCAN1.4 in (N) soleus and (O) EDL muscles in control and Herpud1 KO mice (mean ± SEM; $n = 3$). $^{***}p < 0.001$ between insulin stimulated conditions after one-way ANOVA followed by Tukey's *post hoc* test.

### 2.9. 2-NBD-glucose (2-NBDG) uptake

L6 myotubes grown on glass coverslips were serum-starved for 3 h, stimulated with insulin 100 nM for 20 min, and incubated with 2-NBDG (300 μM) for 15 min at 37 °C, as previously described [20]. Cells were transferred to an Olympus Disk Scanning Unit (DSU) confocal microscope (Olympus). Images were quantified using ImageJ software (NIH).

### 2.10. GLUT4 translocation assay (OPD assay)

An absorbance-based immunoassay was used to determine GLUT4 translocation as previously reported [19,20]. Briefly, L6 GLUT4-myc myotubes in 12-well plates were fixed with paraformaldehyde 4% (v/v) for 10 min, quenched with glycine solution (100 mM) for 10 min, and blocked with 5% (p/v) BSA solution for 1 h. Myotubes were then incubated with anti-Myc antibody (1:500) overnight at 4 °C, washed 5 times with PBS, and incubated with goat anti-rabbit secondary antibody (1:1000) for 1 h at 4 °C. After washing 5 times with PBS, cells were incubated with *o*-phenylenediamine (OPD) solution until a yellow-red color was generated. Absorbance was measured at 492 nm in a GloMax multi-detection system plate reader (Promega Corporation).

### 2.11. Western blot analysis

Protein immunodetection was performed as previously described [10], with overnight incubation with primary antibodies at 4 °C and 1 h incubation with secondary antibodies at room temperature, followed by incubation with EZ-ECL-enhanced chemiluminescence according to manufacturer indications. Readings were normalized to β-tubulin or GAPDH. Densitometric analysis was performed with ImageJ (NIH).

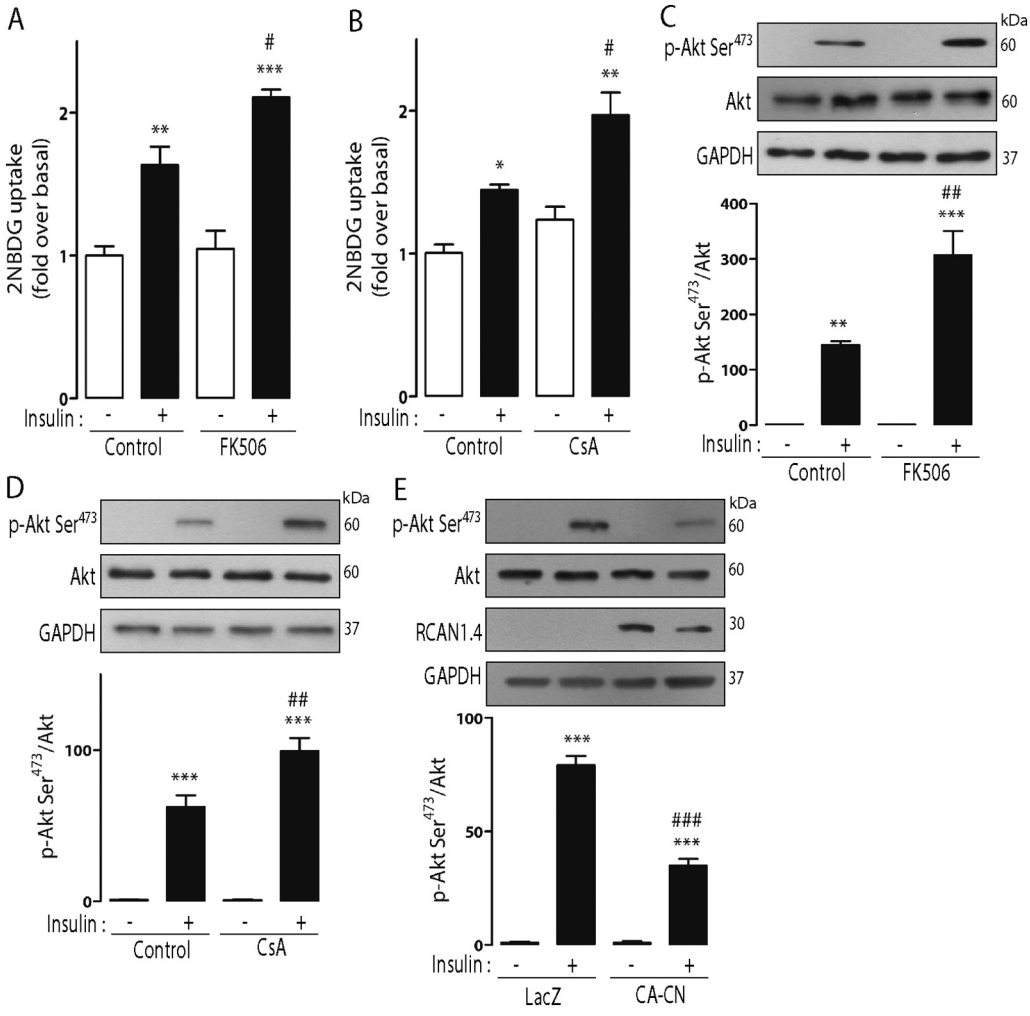


**Fig. 5.** Calcineurin regulates Akt Ser$^{473}$ phosphorylation and glucose uptake in L6 myotubes. (A) Effect of FK506 in 2-NBDG uptake on L6 cells. Cells were pre-incubated with FK506 100 nM for 30 min prior to insulin stimulation for 20 min (mean ± SEM; $n = 3$). (B) Effect of CsA in 2-NBDG uptake. L6 myotubes were pre-incubated with CsA 5 μM for 30 prior to insulin stimulation for 20 min (mean ± SEM; $n = 3$). (C) Top panel: Effect of FK506 on Akt Ser$^{473}$ phosphorylation (representative image). Bottom panel: Immunoblot quantification (mean ± SEM; $n = 3$). (D) Top panel: Representative Western blot showing the effect of CsA on Akt Ser$^{473}$ phosphorylation. Bottom panel: Densitometric analysis (mean ± SEM; $n = 3$). (E) Top panel: Representative Western blot showing the effect of the constitutively-active form of calcineurin (CA-CN) on Akt Ser$^{473}$ phosphorylation in muscle cells. Bottom panel: Quantification of Akt Ser$^{473}$ phosphorylation (mean ± SEM; $n = 4$). $^{*}p < 0.05$, $^{**}p < 0.01$, $^{***}p < 0.001$ between basal conditions. $^{\#}p < 0.05$, $^{\#\#}p < 0.01$ and $^{\#\#\#}p < 0.001$ between insulin-stimulated conditions after one-way ANOVA followed by Tukey's *post hoc* test.

### 2.12. Cytosolic $Ca^{2+}$ measurement

L6 cells were grown and differentiated on 25-mm coverslips. Myotubes were preloaded with the fluorescent $Ca^{2+}$ indicators fluo-4 AM or fura-2 AM (5 μM) at 37 °C for 30 min in Krebs-Ringer buffer [145 mM NaCl; 5 mM KCl; 2.6 mM $MgCl_2$; 1 mM $CaCl_2$; 10 mM HEPES-Na; 5.6 mM D-glucose; pH 7.4]. For experiments without external $Ca^{2+}$, $CaCl_2$ was omitted and 0.1 mM EGTA was added to Krebs-Ringer buffer. Cells were then washed with Krebs-Ringer buffer, mounted in a 1-mL metal chamber, and transferred to an Olympus Disk Scanning Unit (DSU) confocal microscope (Olympus). Cells loaded with fluo-4 AM were excited at 488 nm, and images were collected every 1 s. Cells loaded with fura-2 AM were excited alternately at 340/380 nm, and images were collected every 2 s.

### 2.13. Mitochondrial $Ca^{2+}$ measurement

L6 cells were preloaded with rhod-FF AM (5 μM) at 37 °C for 30 min in Krebs-Ringer buffer as previously described [21]. Myotubes were washed 30 min in Krebs-Ringer buffer before measurement. Excitation was performed at 568 nm, and images were collected every 1 s. Mitopericam experiments were performed as previously described [11]. Cells were excited at 405 nm, and images were collected every 1 s.

### 2.14. Cell viability

Viability was determined by measuring incorporation of the vital dye propidium iodide (PI) (1 μg/mL) as previously described [8,22]. PI fluorescence was quantified in a BD Accuri C6 flow cytometer (BD Biosciences).

### 2.15. Statistical analysis

Data shown are the mean ± SEM of at least three independent experiments and represent experiments performed on at least three separate occasions with similar outcomes. Data were analyzed using Student's *t*-test or one-way ANOVA, and comparisons between groups were performed using a protected Tukey's test. Statistical significance was defined as $p < 0.05$.

## 3. Results and discussion

### 3.1. Herpud1 regulates insulin-dependent glucose uptake in L6 myotubes

Insulin stimulates glucose uptake in skeletal muscle by increasing GLUT4 glucose transporter translocation to the plasma membrane [23]. The signaling pathway that regulates GLUT4 involves activation of serine/threonine kinase Akt, a critical node in this pathway [24]. Our results showed that 100 nM insulin was the lowest dose to induce activation of insulin signaling pathway and glucose uptake in L6 myotubes (Supplementary Fig. 1). This dose of insulin has been widely used in the study of the insulin signaling in L6 cells [10,11,20]. To test the role of Herpud1 in glucose uptake, we depleted Herpud1 using a specific small interfering RNA (siHerpud1) in rat-derived skeletal muscle cell line L6 differentiated to myotubes (Fig. 1A). Herpud1 knockdown did not alter myotube area, differentiation markers, or viability

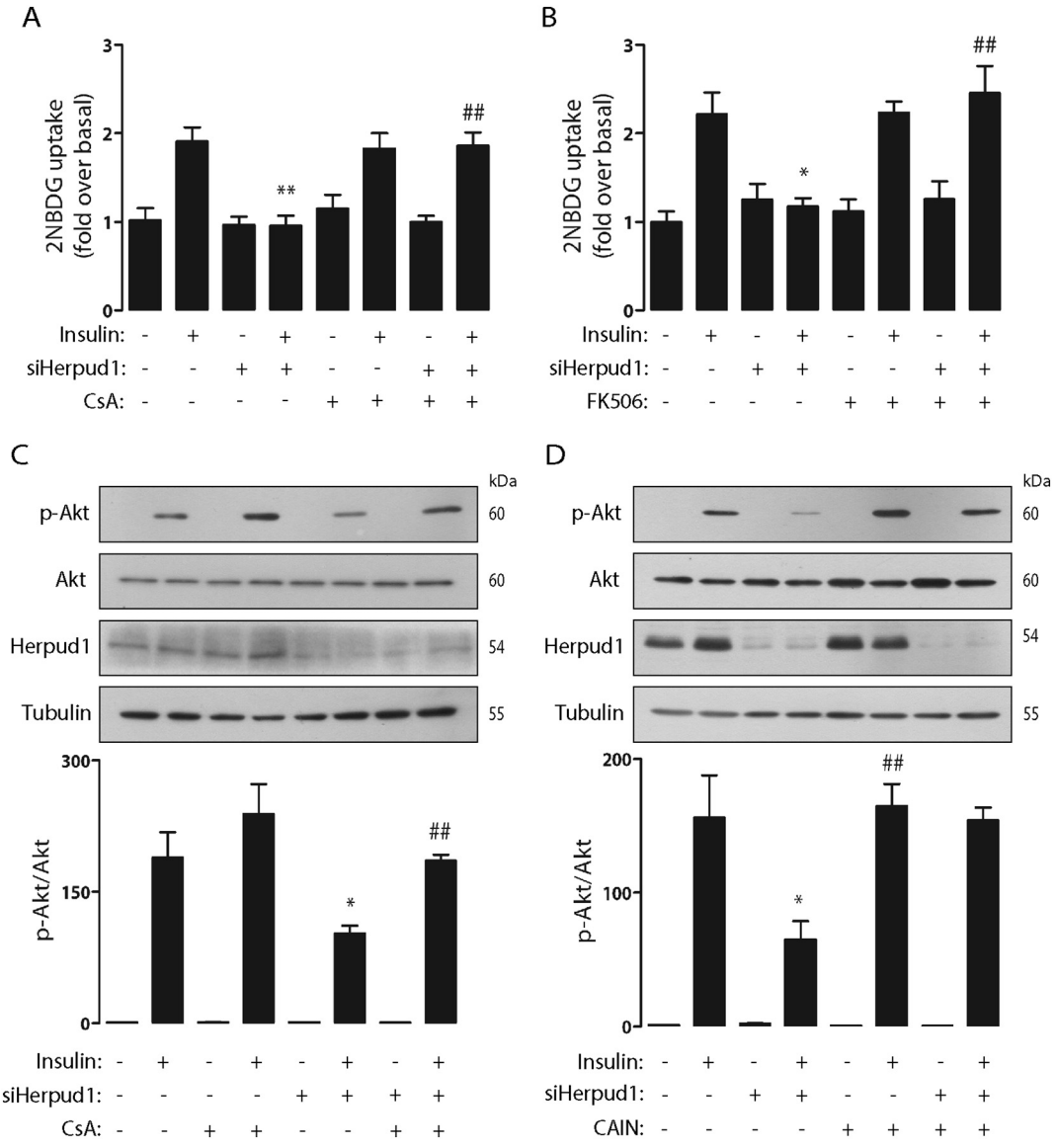


**Fig. 6.** Calcineurin inhibition restores insulin signaling in Herpud1-knockdown muscle cells. (A) Effect of 30 min pre-incubation with CsA (5 μM) on 2-NBDG uptake in control and Herpud1-depleted muscle cells (mean ± SEM; $n = 3$). $^{**}p < 0.01$ between bars 2 and 4; $^{\#\#}p < 0.01$ between bars 4 and 8 after one-way ANOVA followed by Tukey's *post hoc* test. (B) Effect of 30 min pre-incubation with FK506 100 nM on 2-NBDG uptake in siControl and siHerpud1 L6 myotubes (mean ± SEM; $n = 3$). $^{*}p < 0.05$ between bars 2 and 4; $^{\#\#}p < 0.01$ between bars 4 and 8 after one-way ANOVA followed by Tukey's *post hoc* test. (C) Top panel: CsA restores insulin-triggered Akt $Ser^{473}$ phosphorylation in siHerpud1 L6 myotubes (representative image). Bottom panel: Densitometric quantification (mean ± SEM; $n = 3$). $^{*}p < 0.05$ between bars 2 and 6; $^{\#\#}p < 0.01$ between bars 6 and 8 after one-way ANOVA followed by Tukey's *post hoc* test. (D) Top panel: Representative Western blot showing the effect of CAIN overexpression on Akt $Ser^{473}$ phosphorylation in control and Herpud1-depleted cells. Bottom panel: Data quantification (mean ± SEM; $n = 3$). $^{*}p < 0.05$ between bars 2 and 4; $^{\#\#}p < 0.01$ between bars 4 and 6 after one-way ANOVA followed by Tukey's *post hoc* test.

(Supplementary Fig. 2). Previously, we showed increased autophagy levels in Herpud1-depleted HeLa cells under glucose deprivation [22]. However, no differences in autophagy markers were found in Herpud1 knockdown skeletal muscle cells (Supplementary Fig. 3). Our results showed that Herpud1 silencing significantly decreased insulin-stimulated glucose uptake, without altering basal glucose incorporation (Fig. 1B and C). Next, we assessed the presence of GLUT4 inserted at the plasma membrane under basal (non-stimulated) and insulin-stimulated conditions through OPD assay [19,20]. Herpud1 knockdown decreased insulin-dependent GLUT4 translocation to the plasma membrane without affecting basal surface GLUT4 levels (Fig. 1D) or total GLUT4 levels (Supplementary Fig. 2C). Moreover, Herpud1 depletion significantly decreased insulin-induced Akt $Ser^{473}$ phosphorylation (Fig. 1E). Akt phosphorylation at the $Ser^{473}$ residue is necessary for its full activation [25]. Interestingly, PDK1-dependent phosphorylation of Akt at $Thr^{308}$ residue was not affected, suggesting a specific mechanism of Akt regulation at $Ser^{473}$ residue (Fig. 1F) [26,27]. Insulin-induced GLUT4 translocation to plasma membrane in skeletal muscle requires the Akt-dependent phosphorylation and inhibition of Rab-GAP protein TBC1D4 [28]. In accordance with previously described results, siHerpud1 decreases TBC1D4 $Thr^{642}$ phosphorylation in L6 myotubes (Fig. 1G). Additionally, this siHerpud1 also decreased Akt-dependent phosphorylation of mTOR $Ser^{2448}$ (Fig. 1H), FOXO3a$^{Thr32}$ (Fig. 1I) and S6 $Ser^{235/236}$ (Fig. 1J) [29–31]. Conversely, Herpud1 knockdown did not alter insulin receptor (IR) $Tyr^{1361}$ phosphorylation (Supplementary Fig. 4A), suggesting that alterations in insulin signaling occur downstream of IR. Physical exercise induces glucose uptake through a signaling pathway that involves AMPK activation [32]. Our results showed that Herpud1 silencing did not change AMPK $Thr^{172}$ phosphorylation, suggesting that AMPK activation was not altered in our model (Supplementary Fig. 4B).

To corroborate the in vivo role of Herpud1 in insulin signaling, we

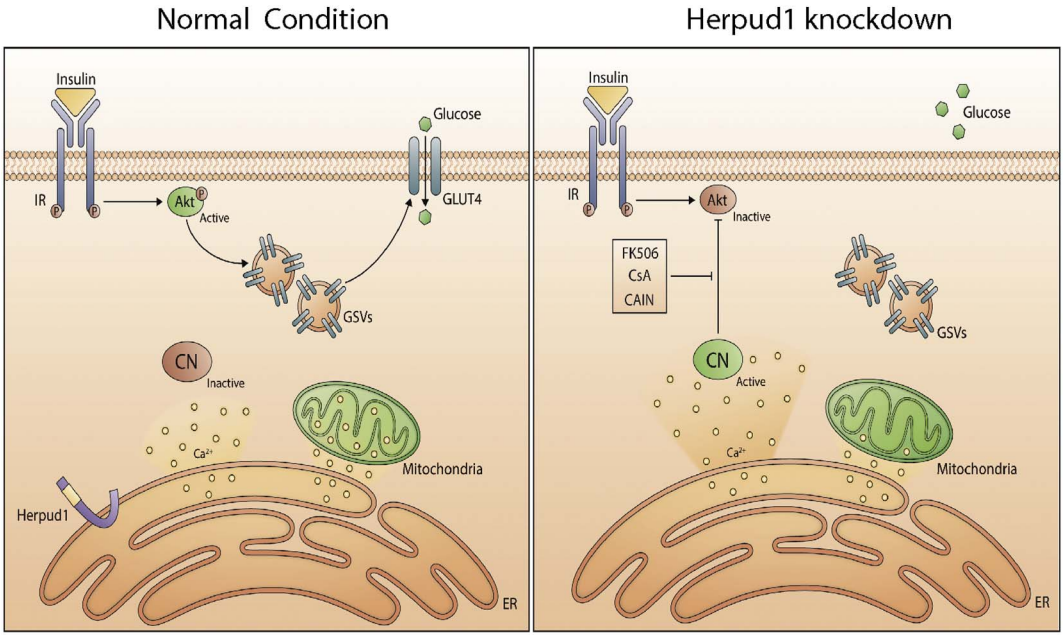


**Fig. 7.** Proposed model. Left panel: Under normal conditions, Herpud1 maintains adequate $IP_3R$-dependent $Ca^{2+}$ homeostasis, controlling calcineurin activity. In this context, insulin-induced Akt phosphorylation and downstream signaling occurs normally. Right panel: Herpud1 depletion alters intracellular $Ca^{2+}$ homeostasis. In Herpud1-knockdown cells, $IP_3R$-induced mitochondrial $Ca^{2+}$ uptake decreases, while cytosolic $Ca^{2+}$ response increases, leading to increased $Ca^{2+}$-dependent serine-threonine phosphatase calcineurin activity. Calcineurin decreases Akt phosphorylation and blunts downstream insulin signaling. Furthermore, calcineurin inhibition restores insulin signaling in Herpud1-depleted L6 cells.

examined skeletal muscles from whole-body *Herpud1*-KO mice. C57BL/6 wild-type (control) and *Herpud1*-KO mice were intraperitoneally injected with 1 U/Kg insulin as previously described [17,18], and *soleus* and *extensor digitorum longus* (EDL) muscles were isolated for Western blot analysis. There was a statistically-significant decrease in insulin-induced Akt $Ser^{473}$ phosphorylation in the soleus muscle of *Herpud1*-KO mice (Fig. 2A and B). This result was not replicated in EDL muscle (Fig. 2D and E), suggesting a major influence of Herpud1 in oxidative muscles. No differences in IR $Tyr^{1361}$ phosphorylation were observed (Fig. 2A, C, D, and F). The implications of decreased Akt $Ser^{473}$ phosphorylation in *soleus* muscle of *Herpud1*-KO mice in insulin signaling downstream of Akt and in glucose uptake are unknown and should be investigated in the future.

The loss-of-function approach was complemented by examining the effect of Herpud1 overexpression on insulin response in L6 myotubes (Fig. 3A). Overexpressed Herpud1-GFP showed a pattern consistent with ER localization in L6 myoblasts (Fig. 3A). Notably, insulin-dependent glucose uptake was potentiated in myotubes transfected with a plasmid encoding the mouse Herpud1 gene (Fig. 3B). These findings are consistent with significantly increased Akt $Ser^{473}$ (Fig. 3C) and S6 $Ser^{235/236}$ (Fig. 3D) phosphorylation, without changes in IR $Tyr^{1361}$ phosphorylation (Supplementary Fig. 4C). Taken together, these findings support a role for Herpud1 in insulin-induced glucose uptake in skeletal muscle cells. To our knowledge, this is the first report describing the role of Herpud1 in skeletal muscle.

Based on our results, we also propose that pharmacological modulation of Herpud1 is a potential target for treating insulin resistance. Interestingly, McLaughlin et al. previously demonstrated that 4-trifluoromethyl-celecoxib, a celecoxib analogue with low affinity for COX-2, selectively upregulates Herpud1 [33]. 4-Trifluoromethyl-celecoxib has shown promising results in animal models of arthritis and neuroinflammation, suggesting that this drug may be useful as a Herpud1 regulator in skeletal muscle [33–35].

### *3.2. Role of Herpud1 in intracellular $Ca^{2+}$ signaling and calcineurin activity in L6 cells*

Next, we focused on understanding the molecular mechanisms underlying the altered insulin response in Herpud1-depleted cells. Previous studies have shown that Herpud1 protects against cell death by stabilizing $IP_3R$-dependent $Ca^{2+}$ signaling under stress conditions [6–8]. To test the role of Herpud1 in $Ca^{2+}$ homeostasis in L6 myotubes, we measured basal and histamine-induced cytosolic and mitochondrial $Ca^{2+}$ responses, given that histamine stimulates $IP_3R$-dependent $Ca^{2+}$ release from the ER [12]. Using fura-2 AM as a cytosolic $Ca^{2+}$ indicator, we observed that Herpud1 knockdown significantly increases the histamine-dependent $Ca^{2+}$ peak response (Fig. 4A–C). Comparable results were observed using fluo-4 AM as a cytosolic $Ca^{2+}$ sensor (Supplementary Fig. 5A–C). Parallel experiments done in the absence of external $Ca^{2+}$ also showed an increased histamine-dependent $Ca^{2+}$ response in Herpud1 knockdown cells (Supplementary Fig. 5G–I). Interestingly, kinetics in absence of external $Ca^{2+}$ showed a slow increase in intracellular $Ca^{2+}$ in response to histamine, suggesting a role for extracellular $Ca^{2+}$ in initial response. This slow $Ca^{2+}$ response via $IP_3Rs$ has been previously described in skeletal muscle cells, and associated to changes in gene expression [36,37]. These findings are consistent with the heightened $Ca^{2+}$ response in Herpud1-depleted cells observed under stress conditions [6,8]. Consistent with these results, a decrease in cytosolic $Ca^{2+}$ signal induced by histamine was observed in L6 myotubes overexpressing Herpud1 (Fig. 4G–I). We also measured the mitochondrial $Ca^{2+}$ response using the genetically-encoded $Ca^{2+}$ indicator mito-pericam. Interestingly, in contrast to its effect on cytosolic $Ca^{2+}$, Herpud1 silencing actually decreased the histamine-dependent mitochondrial $Ca^{2+}$ response (Fig. 4D–F). Similar results were observed when rhod-FF AM was used as a mitochondrial $Ca^{2+}$ indicator (Supplementary Fig. 5D–F). We have previously reported an increased histamine-triggered mitochondrial $Ca^{2+}$ response in Herpud1-knockdown Hela cells [8]. These discrepancies in mitochondrial $Ca^{2+}$ response may be related to cell-specific actions of Herpud1, and future studies are needed to clarify this point. Previous works showed that Herpud1 modulates $Ca^{2+}$ signals by controlling the degradation of $IP_3Rs$ in PC12 cells [6], HeLa cells [8] and cardiac myocytes [38]. Here we show that Herpud1 silencing does not alter the levels of $IP_3R$ isoforms 1, 2 and 3 in L6 myotubes (Fig. 4J and K). Similar results were observed using a pan-$IP_3R$ antibody (Supplementary Fig. 5J). Collectively, these results suggest that Herpud1 regulates $IP_3R$ dependent

$Ca^{2+}$ signals in skeletal muscle cells through a mechanism that does not involve changes in $IP_3R$ protein levels. At this point, we hypothesize that Herpud1 could be necessary for the correct formation of ER-mitochondria contact sites. Mitochondrial $Ca^{2+}$ influx through inner mitochondrial membrane occurs via mitochondrial calcium uniporter (MCU) [39]. Due to the low affinity of MCU for $Ca^{2+}$, mitochondrial $Ca^{2+}$ uptake occurs in microdomains of high $Ca^{2+}$ concentration, which are generated in the sites of proximity between mitochondria and ER calcium release channels [40,41]. Diverse proteins helps to maintain the proximity between the two organelles [42]. Therefore, a defective ER-mitochondria communication in siHerpud1 L6 cells could explain the decreased mitochondrial $Ca^{2+}$ response induced by histamine. On the other hand, mitochondria also modulates amplitude and duration of cytosolic $Ca^{2+}$ responses by buffering ER-generated $Ca^{2+}$ signals in skeletal muscle cells [21]. Thus, decreased $Ca^{2+}$ uptake in the mitochondria could increase cytosolic $Ca^{2+}$ response. Such possibility needs to be studied in the future studies.

Based on these results, we propose that the net increase in the cytosolic calcium response in Herpud1-knockdown cells alters the regulation of $Ca^{2+}$-dependent signaling pathways in the cytosol. Consistent with this hypothesis, we observed that Herpud1 depletion increased RCAN1.4 protein expression in L6 myotubes (Fig. 4L) without changes in the protein levels of the catalytic Aα subunit of calcineurin (Fig. 4M). A similar increase in RCAN1.4 was observed in soleus muscle of *Herpud1*-KO mice (Fig. 4N), without differences between conditions in EDL muscle (Fig. 4O). RCAN1.4 expression is induced by $Ca^{2+}$-dependent serine/threonine phosphatase calcineurin [43]. Moreover, Ni et al. have previously shown that calcineurin interacts with Akt and decreases Akt phosphorylation in cardiomyocytes [14]. Taken together, these results lead us to hypothesize that Herpud1 knockdown blunts the insulin-dependent response through increased phosphatase calcineurin activity in L6 myotubes.

### 3.3. Calcineurin regulates Akt phosphorylation and glucose uptake in L6 myotubes

To investigate whether calcineurin regulates the insulin response in skeletal muscle cells, we assessed the participation of calcineurin in basal and insulin-dependent glucose uptake and Akt $Ser^{473}$ phosphorylation in L6 myotubes. The results showed that pre-incubation of L6 myotubes for 30 min with the calcineurin inhibitors FK506 (100 nM) and cyclosporine A (CsA, 5 μM) increased insulin-induced glucose uptake (Fig. 5A and B) and Akt $Ser^{473}$ phosphorylation (Fig. 5C and D). Conversely, overexpression of a constitutively-active form of calcineurin (CA-CN) decreased insulin-induced Akt $Ser^{473}$ phosphorylation (Fig. 5E). These results suggest that calcineurin plays an important role in insulin signaling in skeletal muscle cells. Based on these results, we propose that increased calcineurin activity in Herpud1-depleted myotubes may affect insulin signaling.

### 3.4. Calcineurin inhibition restores insulin signaling in Herpud1-knockdown L6 myotubes

To directly assess the participation of calcineurin in the abnormal insulin signaling observed in Herpud1-knockdown cells, we measured the effect of calcineurin inhibition on the insulin response of siHerpud1-treated L6 myotubes. Our results show that 30 min of pre-incubation with CsA and FK506 restored insulin-dependent glucose uptake in Herpud1-knockdown L6 cells (Fig. 6A and B). Furthermore, pre-incubation with the calcineurin inhibitor CsA restored insulin-induced Akt $Ser^{473}$ phosphorylation in Herpud1-depleted L6 myotubes (Fig. 6C). A similar restoration of insulin-induced Akt $Ser^{473}$ phosphorylation was attained with overexpression of the endogenous calcineurin inhibitor protein CAIN (Fig. 6D). We observed a complete inhibition of insulin-induced glucose uptake in siHerpud1 cells (Fig. 6A–B) but a partial effect in Fig.1C. These discrepancies could be explained by small differences in the extension of Herpud1 silencing or by differences in experimental conditions between both experiments. Moreover, the complete inhibition of glucose uptake in siHerpud1 L6 myotubes (Fig. 6A–B) was accompanied by only a partial decrease in Akt $Ser^{473}$ phosphorylation (Fig. 6C–D). We hypothesize that the level of Akt activation in siHerpud1 L6 cells is insufficient to trigger a significant increase in glucose uptake in these experiments. However we cannot rule out that Herpud1 may regulate other unknown pathway necessary for insulin-induced glucose uptake.

Based on these findings, we conclude that calcineurin also represents a potential target for intervention in skeletal muscle insulin resistance. A recent study has shown that skeletal muscle-specific ablation of calcineurin protects against obesity and metabolic alterations induced by a high-fat diet [44]. Although high doses of calcineurin inhibitors increase the risk of obesity and diabetes in patients [45], there is emerging evidence that low-dose treatment can have positive effects on metabolism, suggesting novel clinical applications for these drugs [46].

The main limitations of the present study are: a) We presented limited data on skeletal muscle from the mice. Future studies should include data on glucose uptake and signaling (phosphorylation of Akt on Ser473 and Thr308 and phosphorylation of TBC1D4 on Thr642) in the WT and KO soleus and EDL muscles that are studied under ex vivo conditions with controlled, physiologic insulin doses. The direct role of $Ca^{2+}$-calcineurin on insulin response should also be demonstrated in skeletal muscle of Herpud1-KO mice. Moreover, considering that in *soleus* muscle of mice predominate oxidative fiber types [47], which represents a limited portion of total muscle fibers, the overall impact of Herpud1 deletion in insulin sensitivity requires further investigation in a physiological context. b) Further studies are also necessary to understand the role of Herpud1 on the insulin response in pathological models of obesity and insulin resistance. These investigations should explore the role of Herpud1 on insulin sensitivity in tissue-specific knockout animals both in ex vivo and in vivo conditions.

Finally, we conclude that Herpud1 regulates the insulin response in skeletal muscle through $Ca^{2+}$/calcineurin-dependent modulation of Akt phosphorylation, providing a new perspective for insulin resistance in muscle cells (Fig. 7).

## Conflicts of interest

There are no potential conflicts of interest relevant to this article to report.

## Funding

This work was supported by Fondo Nacional de Investigación Científica y Tecnológica (FONDECYT) grants 1161156 to S.L. and 11130285 to R.T. Redes 170032 to M.C. and Fondo de Financiamiento de Centros de Investigación en Áreas Prioritarias (FONDAP) grant 15130011 to S.L., M.C., L.G. and R.T. M.N.-M. was supported by a PhD Fellowship from the Comisión Nacional de Investigación Científica y Tecnológica (CONICYT), Chile.

## Transparency document

The Transparency document associated with this article can be found, in online version.

## Acknowledgements

The authors thank Fidel Albornoz and Gindra Latorre (Faculty of Chemical & Pharmaceutical Sciences, University of Chile) for their excellent technical assistance.

## Appendix A. Supplementary data

Supplementary data to this article can be found online at https://doi.org/10.1016/j.bbadis.2018.02.018.

## References


[1] R.A. DeFronzo, D. Tripathy, Skeletal muscle insulin resistance is the primary defect in type 2 diabetes, Diabetes Care 32 (Suppl. 2) (2009).

[2] K. Kokame, K.L. Agarwala, H. Kato, T. Miyata, Herp, a new ubiquitin-like membrane protein induced by endoplasmic reticulum stress, J. Biol. Chem. 275 (2000) 32846–32853.

[3] T. van Laar, T. Schouten, E. Hoogervorst, M. van Eck, A.J. van der Eb, C. Terleth, The novel MMS-inducible gene Mif1/KIAA0025 is a target of the unfolded protein response pathway, FEBS Lett. 469 (2000) 123–131.

[4] Y. Eura, H. Yanamoto, Y. Arai, T. Okuda, T. Miyata, K. Kokame, Derlin-1 deficiency is embryonic lethal, Derlin-3 deficiency appears normal, and Herp deficiency is intolerant to glucose load and ischemia in mice, PLoS One 7 (2012) e34298.

[5] W.R. Frontera, J. Ochala, Skeletal muscle: a brief review of structure and function, Calcif. Tissue Int. 96 (2015) 183–195.

[6] C. Belal, N.J. Ameli, A. El kommos, S. Bezalel, A.M. Al'Khafaji, M.R. Mughal, M.P. Mattson, G.A. Kyriazis, B. Tyrberg, S.L. Chan, The homocysteine-inducible endoplasmic reticulum (ER) stress protein herp counteracts mutant alpha-synuclein-induced ER stress via the homeostatic regulation of ER-resident calcium release channel proteins, Hum. Mol. Genet. 21 (2012) 963–977.

[7] S.L. Chan, W. Fu, P. Zhang, A. Cheng, J. Lee, K. Kokame, M.P. Mattson, Herp stabilizes neuronal $Ca^{2+}$ homeostasis and mitochondrial function during endoplasmic reticulum stress, J. Biol. Chem. 279 (2004) 28733–28743.

[8] F. Paredes, V. Parra, N. Torrealba, M. Navarro-Marquez, D. Gatica, R. Bravo-sagua, R. Troncoso, C. Pennanen, C. Quiroga, M. Chiong, C. Caesar, W.R. Taylor, J. Molgó, A. San, E. Jaimovich, S. Lavandero, HERPUD1 protects against oxidative stress-induced apoptosis through downregulation of the inositol 1, 4, 5-trisphosphate receptor, Free Radic. Biol. Med. 90 (2016) 206–218.

[9] A.E. Contreras-Ferrat, B. Toro, R. Bravo, V. Parra, C. Vasquez, C. Ibarra, D. Mears, M. Chiong, E. Jaimovich, A. Klip, S. Lavandero, An inositol 1,4,5-triphosphate (IP3)-IP3 receptor pathway is required for insulin-stimulated glucose transporter 4 translocation and glucose uptake in cardiomyocytes, Endocrinology 151 (2010) 4665–4677.

[10] A. del Campo, V. Parra, C. Vasquez-Trincado, T. Gutiérrez, P.E. Morales, C. López-Crisosto, R. Bravo-Sagua, M.F. Navarro-Marquez, H.E. Verdejo, A. Contreras-Ferrat, R. Troncoso, M. Chiong, S. Lavandero, Mitochondrial fragmentation impairs insulin-dependent glucose uptake by modulating Akt activity through mitochondrial $Ca^{2+}$ uptake, Am. J. Physiol. Endocrinol. Metab. 306 (2014) E1–E13.

[11] A. Contreras-Ferrat, P. Llanos, C. Vásquez, A. Espinosa, C. Osorio-Fuentealba, M. Arias-Calderon, S. Lavandero, A. Klip, C. Hidalgo, E. Jaimovich, Insulin elicits a ROS-activated and an $IP_3$-dependent $Ca^{2+}$ release, which both impinge on GLUT4 translocation, J. Cell Sci. 127 (2014) 1911–1923.

[12] T. Gutiérrez, V. Parra, R. Troncoso, C. Pennanen, A. Contreras-Ferrat, C. Vasquez-Trincado, P.E. Morales, C. Lopez-Crisosto, C. Sotomayor-Flores, M. Chiong, B. a Rothermel, S. Lavandero, Alteration in mitochondrial $Ca^{2+}$ uptake disrupts insulin signaling in hypertrophic cardiomyocytes, Cell Commun. Signal. 12 (2014) 68.

[13] H. Li, A. Rao, P.G. Hogan, Interaction of calcineurin with substrates and targeting proteins, Trends Cell Biol. 21 (2011) 91–103.

[14] Y.G. Ni, N. Wang, D.J. Cao, N. Sachan, D.J. Morris, R.D. Gerard, M. Kuro-O, B.A. Rothermel, J.A. Hill, FoxO transcription factors activate Akt and attenuate insulin signaling in heart by inhibiting protein phosphatases, Proc. Natl. Acad. Sci. U. S. A. 104 (2007) 20517–20522.

[15] A. Musarò, K.J. McCullagh, F.J. Naya, E.N. Olson, N. Rosenthal, IGF-1 induces skeletal myocyte hypertrophy through calcineurin in association with GATA-2 and NF-ATc1, Nature 400 (1999) 581–585.

[16] C. Semsarian, M.-J. Wu, Y.-K. Ju, T. Marciniec, T. Yeoh, D.G. Allen, R.P. Harvey, R.M. Graham, Skeletal muscle hypertrophy is mediated by a $Ca^{2+}$-dependent calcineurin signalling pathway, Nature 400 (1999) 576–581.

[17] C.S. Lee, A. Dagnino-Acosta, V. Yarotskyy, A. Hanna, A. Lyfenko, M. Knoblauch, D.K. Georgiou, R.A. Poché, M.W. Swank, C. Long, I.I. Ismailov, J. Lanner, T. Tran, K. Dong, G.G. Rodney, M.E. Dickinson, C. Beeton, P. Zhang, R.T. Dirksen, S.L. Hamilton, Ca(2+) permeation and/or binding to CaV11 fine-tunes skeletal muscle Ca(2+) signaling to sustain muscle function, Skelet. Muscle 5 (2015) 4.

[18] O.P. McGuinness, J.E. Ayala, M.R. Laughlin, D.H. Wasserman, NIH experiment in centralized mouse phenotyping: the Vanderbilt experience and recommendations for evaluating glucose homeostasis in the mouse, Am. J. Physiol. Endocrinol. Metab. 297 (2009) E849–E855.

[19] Q. Wang, Z. Khayat, K. Kishi, Y. Ebina, A. Klip, Glut4 translocation by inslin in intact muscle cells: indection by a fast and quantitivative assay, FEBS Lett. 427 (1998) 193–197.

[20] C. Osorio-Fuentealba, A.E. Contreras-Ferrat, F. Altamirano, A. Espinosa, Q. Li, W. Niu, S. Lavandero, A. Klip, E. Jaimovich, Electrical stimuli release ATP to increase GLUT4 translocation and glucose uptake via PI3Kγ-Akt-AS160 in skeletal muscle cells, Diabetes 62 (2013) 1519–1526.

[21] V. Eisner, V. Parra, S. Lavandero, C. Hidalgo, E. Jaimovich, Mitochondria fine-tune the slow $Ca^{2+}$ transients induced by electrical stimulation of skeletal myotubes, Cell Calcium 48 (2010) 358–370.

[22] C. Quiroga, D. Gatica, F. Paredes, R. Bravo, R. Troncoso, Z. Pedrozo, A.E. Rodriguez, B. Toro, M. Chiong, J.M. Vicencio, C. Hetz, S. Lavandero, Herp depletion protects from protein aggregation by up-regulating autophagy, Biochim. Biophys. Acta - Mol. Cell Res. 1833 (2013) 3295–3305.

[23] A. Klip, Y. Sun, T.T. Chiu, K.P. Foley, Signal transduction meets vesicle traffic: the software and hardware of GLUT4 translocation, Am. J. Physiol. Cell Physiol. 306 (2014) C879–C886.

[24] C.M. Taniguchi, B. Emanuelli, C.R. Kahn, Critical nodes in signalling pathways: insights into insulin action, Nat. Rev. Mol. Cell Biol. 7 (2006) 85–96.

[25] D.D. Sarbassov, D.A. Guertin, S.M. Ali, D.M. Sabatini, Phosphorylation and regulation of Akt/PKB by the rictor-mTOR complex, Science 307 (2005) 1098–1101.

[26] D. Stokoe, L.R. Stephens, T. Copeland, P.R.J. Gaffney, C.B. Reese, G.F. Painter, A.B. Holmes, F. Mccormick, P.T. Hawkins, Dual role of phosphatidylinositol-3,4,5-triphosphate in the activation of protein kinase B, Science 277 (1997) 567–570.

[27] D.R. Alessi, S.R. James, C.P. Downes, A.B. Holmes, P.R. Gaffney, C.B. Reese, P. Cohen, Characterization of a 3-phosphoinositide-dependent protein kinase which phosphorylates and activates protein kinase Balpha, Curr. Biol. 7 (1997) 261–269.

[28] H. Sano, S. Kane, P. Mîinea, J.M. Asara, W.S. Lane, C.W. Garner, G.E. Lienhard, Insulin-stimulated phosphorylation of a rab GTPase-activating protein regulates GLUT4 translocation, J. Biol. Chem. 278 (2003) 14599–14602.

[29] A. Sekulić, C.C. Hudson, J.L. Homme, P. Yin, D.M. Otterness, L.M. Karnitz, R.T. Abraham, A direct linkage between the phosphoinositide 3-kinase-AKT signaling pathway and the mammalian target of rapamycin in mitogen-stimulated and transformed cells, Cancer Res. 60 (2000) 3504–3513.

[30] A. Brunet, A. Bonni, M.J. Zigmond, M.Z. Lin, P. Juo, L.S. Hu, M.J. Anderson, K.C. Arden, J. Blenis, M.E. Greenberg, Akt promotes cell survival by phosphorylating and inhibiting a forkhead transcription factor, Cell 96 (1999) 857–868.

[31] B. Magnuson, B. Ekim, D.C. Fingar, Regulation and function of ribosomal protein S6 kinase (S6K) within mTOR signalling networks, Biochem. J. 441 (2012) 1–21.

[32] T.E. Jensen, Y. Angin, L. Sylow, E.A. Richter, Is contraction-stimulated glucose transport feedforward regulated by $Ca^{2+}$? Exp. Physiol. 99 (2014) 1562–1568.

[33] M. McLaughlin, I. Alloza, H.P. Quoc, C.J. Scott, Y. Hirabayashi, K. Vandenbroeck, Inhibition of secretion of interleukin (IL)-12/IL-23 family cytokines by 4-trifluoromethyl-celecoxib is coupled to degradation via the endoplasmic reticulum stress protein HERP, J. Biol. Chem. 285 (2010) 6960–6969.

[34] A. Chiba, M. Mizuno, C. Tomi, R. Tajima, I. Alloza, A. di Penta, T. Yamamura, K. Vandenbroeck, S. Miyake, A 4-trifluoromethyl analogue of celecoxib inhibits arthritis by suppressing innate immune cell activation, Arthritis Res. Ther. 14 (2012) 1–10.

[35] A. Di Penta, A. Chiba, I. Alloza, A. Wyssenbach, T. Yamamura, P. Villoslada, S. Miyake, K. Vandenbroeck, A trifluoromethyl analogue of celecoxib exerts beneficial effects in neuroinflammation, PLoS One 8 (2013) 1–15.

[36] M.A. Carrasco, N. Riveros, J. Ríos, M. Müller, F. Torres, J. Pineda, S. Lantadilla, E. Jaimovich, Depolarization-induced slow calcium transients activate early genes in skeletal muscle cells, Am. J. Physiol. Cell Physiol. 284 (2003) C1438–C1447.

[37] M. Casas, R. Figueroa, G. Jorquera, M. Escobar, J. Molgó, E. Jaimovich, $IP_3$-dependent, post-tetanic calcium transients induced by electrostimulation of adult skeletal muscle fibers, J. Gen. Physiol. 136 (2010) 455–467.

[38] N. Torrealba, M. Navarro-Marquez, V. Garrido, Z. Pedrozo, D. Romero, Y. Eura, E. Villalobos, J.C. Roa, M. Chiong, K. Kokame, S. Lavandero, Herpud1 negatively regulates pathological cardiac hypertrophy by inducing IP3 receptor degradation, Sci. Rep. 7 (2017) 13402.

[39] Y. Kirichok, G. Krapivinsky, D.E. Clapham, The mitochondrial calcium uniporter is a highly selective ion channel, Nature 427 (2004) 360–364.

[40] R. Rizzuto, P. Pinton, W. Carrington, F.S. Fay, K.E. Fogarty, L.M. Lifshitz, R.A. Tuft, T. Pozzan, Close contacts with the endoplasmic reticulum as determinants of mitochondrial $Ca^{2+}$ responses close contacts with the endoplasmic reticulum as determinants of mitochondrial $Ca^{2+}$ responses, Science 280 (1998) 1763–1766.

[41] G. Csordás, A.P. Thomas, G. Hajnóczky, Quasi-synaptic calcium signal transmission between endoplasmic reticulum and mitochondria, EMBO J. 18 (1999) 96–108.

[42] S. Marchi, S. Patergnani, P. Pinton, The endoplasmic reticulum-mitochondria connection: one touch, multiple functions, Biochim. Biophys. Acta Bioenerg. 1837 (2014) 461–469.

[43] B.A. Rothermel, R.B. Vega, R.S. Williams, The role of modulatory calcineurin-interacting proteins in calcineurin signaling, Trends Cardiovasc. Med. 13 (2003) 15–21.

[44] P.T. Pfluger, D.G. Kabra, M. Aichler, S.C. Schriever, K. Pfuhlmann, V.C. García, M. Lehti, J. Weber, M. Kutschke, J. Rozman, J.W. Elrod, A.L. Hevener, A. Feuchtinger, M. Hrabě De Angelis, A. Walch, S.M. Rollmann, B.J. Aronow, T.D. Müller, D. Perez-Tilve, M. Jastroch, et al., Calcineurin links mitochondrial elongation with energy metabolism, Cell Metab. 22 (2015) 838–850.

[45] H. Chakkera, Y. Kudva, B. Kaplan, Calcineurin inhibitors: pharmacologic mechanisms impacting both insulin resistance and insulin secretion leading to glucose dysregulation and diabetes mellitus, Clin. Pharmacol. Ther. 101 (2017) 114–120.

[46] Akoulitchev, A., Milway, E., Mellor, E.J., and Youdell, M, Tacrolimus and analogues thereof for medical use, Patent application WO2014188198 A1, (2014).

[47] D. Sandonà, J.-F. Desaphy, G.M. Camerino, E. Bianchini, S. Cicilliot, et al., Adaptation of mice skeletal muscle to long-term microgravity in the MDS mission, PLoS One 7 (2012) 114–120.